

Application of Hertzian Tests to Measure Stress–Strain Characteristics of Ceramics at Elevated Temperatures

Estíbaliz Sánchez-González, Juan J. Meléndez-Martínez, and Antonia Pajares[†]

Departamento de Física, Facultad de Ciencias, Universidad de Extremadura, Badajoz 06071, Spain

Pedro Miranda and Fernando Guiberteau

Departamento de Electrónica e Ingeniería Electromecánica, Escuela de Ingenierías Industriales, Universidad de Extremadura, Badajoz 06071, Spain

Brian R. Lawn

Materials Science and Engineering Laboratory, National Institute of Standards and Technology, Gaithersburg, Maryland 20899-8500

A new method for evaluating the elastic–plastic properties of ceramics from room temperature up to the onset of creep based on Hertzian indentation testing is proposed. Indentation stress–strain curves are compiled for representative alumina and zirconia ceramics at prescribed temperatures. Deconvolution of the indentation stress–strain curves for each material provides a measure of Young’s modulus, yield stress, and work-hardening coefficient as a function of temperature, enabling construction of true stress–strain curves. The stress–strain curves flatten out with increasing temperature, in accordance with an expected increased plastic response at elevated temperatures.

I. Introduction

DESIRABLE MECHANICAL properties of advanced ceramics include high modulus and hardness, and high wear and chemical resistance. Such properties enable ceramics to supplant metals in applications such as bearings, cutting tools, seal valves, and heat exchangers. Any increase of temperature above ambient can significantly affect performance, particularly under contact conditions where local stress levels are uncommonly high. Accordingly, there is a need for a fundamental understanding of the contact properties of ceramics above room temperature, particularly elastic–plastic responses. Indentation studies with spheres are ideally suited to meet this need, because of their experimental simplicity, their amenability to analysis, and (especially) their unique capacity to determine the full elastic–plastic response without premature fracture.¹ Such Hertzian studies have been conducted at room temperature on a wide range of ceramics including alumina, zirconia, silicon nitride, silicon carbide, and dental materials,^{2–7} as well as on thermal barrier coatings and other layer systems.^{8,9} One of the advantages of Hertzian tests is that it covers a range of stresses (from 1 to tens of GPa) and testing size scale (from tens of micrometer to millimeter) not accessible by the more conventional Vickers indentation (stresses above 10 GPa and a scale of micrometer to tens of micrometer) or uniaxial tests (stresses from 1 MPa to 1 GPa and a scale above 1 mm). However, an extension of this testing methodology to high temperatures has not been carried

out. Hertzian tests have been conducted above room temperature for the determination of the temperature dependence of toughness in silicate materials.¹⁰ Routine hot hardness Vickers indentation measurements have also been performed on a wide variety of ceramics.^{11–13} Extensive uniaxial testing and impression creep tests^{14–16} have been conducted on the creep properties of ceramics at very high temperatures. None of these other studies provides a full description of the temperature dependence of the elastic–plastic stress–strain response in the pre-creep region.

The current paper seeks to redress this deficiency. Our aim here is to expand the existing Hertzian testing methodology to deconvolute true stress–strain responses of ceramics from indentation data as a function of temperature. A furnace enables *in situ* indentation testing above room temperature. Commercial polycrystalline alumina and zirconia are used as test materials, with sphere indenters made from the same materials. The deconvolution is carried out using basic elastic–plastic relations in conjunction with finite-element modeling (FEM). Our current focus will be on the methodology, with a more detailed description of material properties deferred to later reports.

II. Experimental Procedure

(1) Materials

Alumina and zirconia were chosen as test materials because their properties have been comprehensively studied in the ceramics literature. The alumina was a commercial polycrystalline material with a grain size of about 6 μm and a porosity of 3% (Goodfellow, Cambridge, U.K.). The zirconia was a commercial Y–TZP containing 5 mol% Y_2O_3 (Imetra, Elmsford, NY). Both materials were supplied as spheres of 3 and 9 mm radius. The spheres were cut in half and used as indenters. Plate specimens for testing were cut from the center regions of the larger spheres to 8 mm thickness and were polished to a 1 μm finish. This procedure ensured that specimen and indenter were always similar materials.

(2) Indentation Tests

Hertzian contact tests were performed using a universal testing machine (Model AG-IS 100 kN, Shimadzu, Kyoto, Japan). A vertical split furnace was incorporated into the testing machine as shown in Fig. 1. The furnace consisted of a cylindrical chamber with a frontal aperture to facilitate specimen access. Upper and lower alumina push rods (40 mm diameter and 350 mm length) were used to support the specimen and deliver the load,

N. Padture—contributing editor

Manuscript No. 21959. Received June 29, 2006; approved August 17, 2006.

This work was funded by the Ministerio de Ciencia y Tecnología (Government of Spain) and the Fondo Social Europeo through grant MAT2003-05584.

[†]Author to whom correspondence should be addressed. e-mail: apajares@unex.es

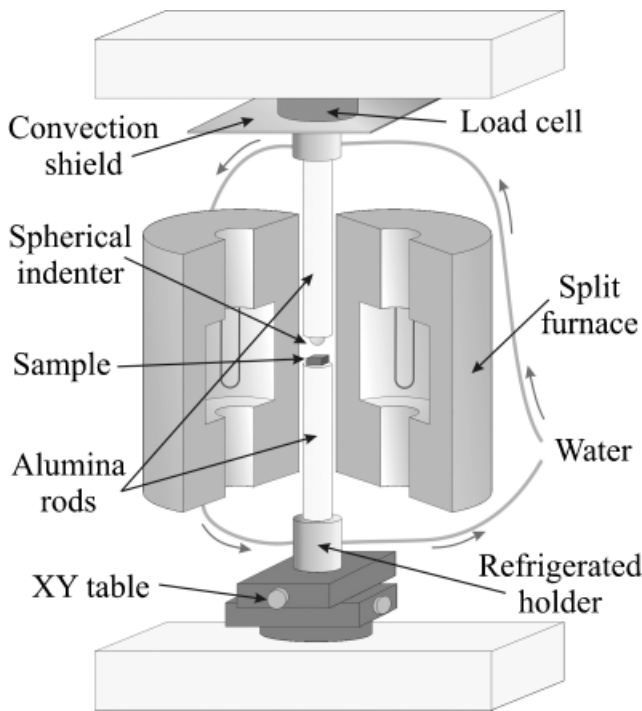


Fig. 1. Schematic of the experimental setup used for the Hertzian tests at elevated temperatures.

with the indenter and specimen at the center of the furnace chamber. The half-sphere indenter and the specimen were, respectively, bonded to the upper and lower push rods using alumina paste (Ceramabond 569, Aremco Products Inc, NY). External push rod holders were cooled with circulating water to protect the load cell. Before bonding the specimen to the rod, a metal film of 50 nm thickness was sputter coated onto the top surface (Polaron SC7640, Quorum Technologies Ltd., New Haven, U.K.), with different metals at different temperatures to provide an optimum imprint of the ensuing indentations—gold at room temperature, rhodium-palladium up to 600°C, and platinum at higher temperatures. The bottom push rod holder was placed on an X–Y table to allow at least 15 tests to be conducted on any specimen at any selected temperature. Indentations were made at a constant crosshead displacement rate of 0.05 mm/min.

Indentation sequences were made at peak loads up to 5000 N in air at temperatures in the range 25°–1200°C for alumina and 25°–1000°C for zirconia. At higher temperatures, creep was observed—data in this region were discarded. The specimens were heated at a rate of 6°C/min, held for 1 h at peak temperature before indentation, and then allowed to cool over several hours by switching off the furnace.

After cooling, contact radius a at each peak load P and indenter radius r were measured by optical microscopy at each indentation site from the contact imprint. Plots of indentation stress ($p_0 = P/\pi a^2$) versus indentation strain (a/r) for each temperature were thereby obtained for each material.

(3) Analysis

Young's modulus E for each prescribed temperature was determined from the linear region of the indentation stress–strain curve using the Hertzian relation for elastic contacts with similar indenters

$$p_0 = [2E/3\pi(1 - \nu^2)]a/r \quad (p_0 < 1.1Y) \quad (1)$$

where ν is Poisson's ratio (generally taken as 0.22 for our materials) and Y is the yield stress.^{1,17,18}

FEM was used to determine yield stress and work-hardening coefficients from the indentation stress–strain curves using AB-AQUS/Standard software (Hibbitt, Karlsson & Sorensen Inc, Pawtucket, RI).¹⁹ The algorithm models a half-sphere indenter of 3 mm radius in axisymmetric contact with a flat specimen, incrementally loaded to prescribed peak loads, with 1 μ m minimum dimension square elements in the near-contact region. Deformation in both the indenter and the specimen is assumed to occur in accordance with a Lüdwig constitutive stress–strain relation²⁰

$$\sigma = E\varepsilon \quad (\sigma < Y) \quad (2a)$$

$$\sigma = Y(E/Y)^n \varepsilon^n \quad (\sigma > Y) \quad (2b)$$

with n being a dimensionless strain-hardening coefficient of value between 0 (fully plastic) and 1 (fully elastic). This model provides a more realistic strain hardening behavior than other simple bilinear models used in previous work,^{19,21–23} without increasing the number of adjustable parameters. For each material at any given temperature, given E from Eq. (1), Y and n are iteratively adjusted to fit the indentation stress–strain data using the algorithm.

III. Results

Figure 2 shows micrographs of the indentation-induced surface damage for a 1500 N load at room temperature and 1000°C for alumina (Fig. 2(a)) and zirconia (Fig. 2(b)). In both materials, the residual impression is markedly larger at the higher temperature, indicating greater deformation. Some ring and radial cracks are observed, most apparent in the zirconia at the higher temperature, but these are considered subsidiary to the greater deformation under the present loading conditions. Some plastic deformation was also observed in the indenter after the tests, especially at the higher temperatures.

Indentation stress–strain curves at temperatures up to 1200°C for alumina and 1000°C for zirconia are shown in Fig. 3. Each point in these curves represents a single indentation performed at a prescribed peak load and temperature. The solid curves through the experimental data are FEM best fits, with appropriately adjusted parameters E , Y , and n for both the test material and the indenter (the latter to allow for observed yield in the indenter). The curves move substantially downward with increasing temperature, as expected. In principle, asymptotic plateaus of these curves at high strain would yield Meyer's hardness of the material at any given temperature. However, in the

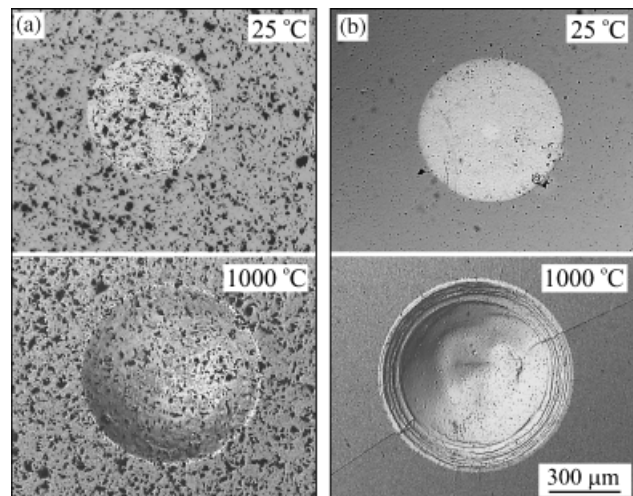


Fig. 2. Optical micrographs showing surface Hertzian damage in (a) alumina and (b) zirconia generated with 3 mm radius indenters of similar materials for 1500 N peak load at room temperature and 1000°C.

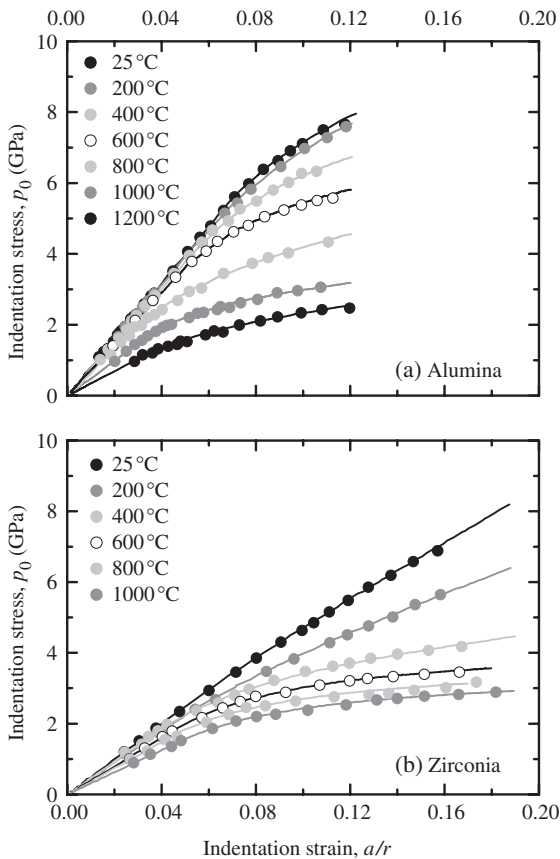


Fig. 3. Indentation stress–strain data for (a) alumina and (b) zirconia at designated temperatures. Hertzian tests were performed with indenters of similar materials of 3 and 9 mm radius (not distinguished here). The solid curves indicate finite-element modeling best fits.

present experiments, we could not reach these plateaus without breaking either the sample or the indenter.

Young’s moduli E obtained from the slopes of the linear region of these curves using Eq. (1) are plotted versus temperature for alumina and zirconia in Fig. 4. Error bars are calculated from the uncertainties in the estimation of the slopes from linear regressions and in most cases are smaller than the size of the symbols, except at higher temperatures, where the number of data points within the elastic region is limited and impression visibility is less clear (Fig. 2). The solid lines through the data points indicate empirical fits. The reduction in E over the tem-

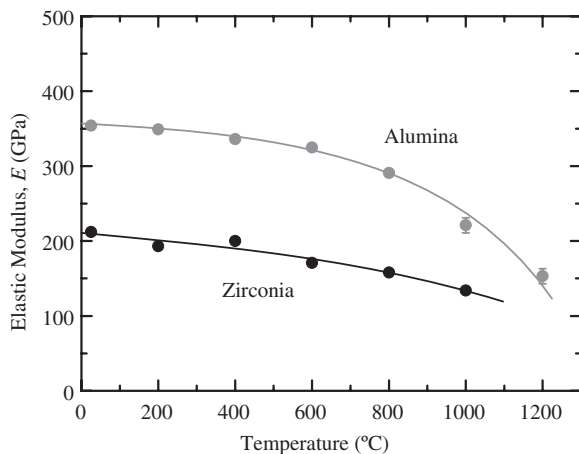


Fig. 4. Young’s modulus E versus temperature for alumina and zirconia. Data points evaluated from slope of the initial linear region of stress–strain curves of Fig. 3 in conjunction with Eq. (1). The solid lines through data indicate empirical fits.

perature range is apparent for both materials, but is especially so for alumina above about 600°C.

Corresponding yield stresses Y and strain-hardening coefficients n obtained from the FEM analyses are plotted as a function of temperature for alumina in Fig. 5(a) and for zirconia in Fig. 5(b). Error bars are estimated uncertainties in the trial FEM calculations, and the solid lines through the data indicate empirical fits. Whereas Y for zirconia diminished relatively slowly and continuously over the temperature range, that for alumina showed an abrupt drop at around 600°C. Closer inspection of the indentation sites revealed some enhanced damage, possibly from enhanced grain boundary degradation in this particular alumina, but this aspect was not investigated in depth. The trends in n show even greater disparities in the two materials, remaining consistently low in the alumina but falling rapidly from near unity in the zirconia. These trends in Y and n , taken together, indicate significant differences in the elastic–plastic responses in the two materials.

IV. Discussion

In this work, we propose a simple Hertzian test methodology to determine the elastic–plastic behavior of ceramics at temperatures up to the onset of creep. Young’s modulus E and yield parameters Y and n are deconvoluted from indentation stress–strain curves using Eqs. (1) and (2), in conjunction with FEM. This information can be used to reconstruct the true stress–strain curve for any given ceramic. Accordingly, in Fig. 6, we plot stress σ versus strain ϵ for our alumina and zirconia by inserting E , Y , and n from Figs. 4 and 5 into Eq. (2). The entire deformation evolution in each material at each temperature, from initial elastic to fully plastic, is now apparent.

These results provide some insights into the deformation processes in the two test ceramics. For the alumina, the curves in the plastic region are relatively flat, consistent with a small, rela-

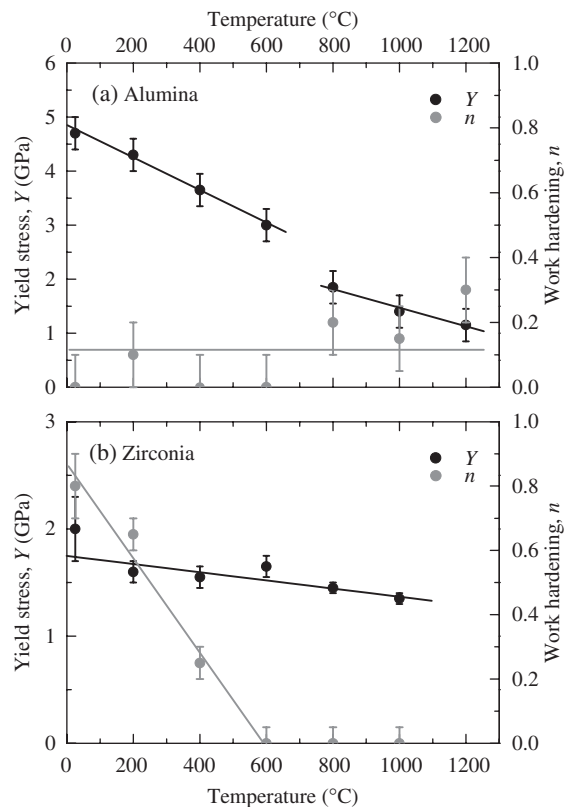


Fig. 5. Yield stress Y and strain-hardening coefficient n versus temperature for (a) alumina and (b) zirconia. Points evaluated by iterative finite element modeling analysis in conjunction with Eq. (2) from stress–strain data of Fig. 3.

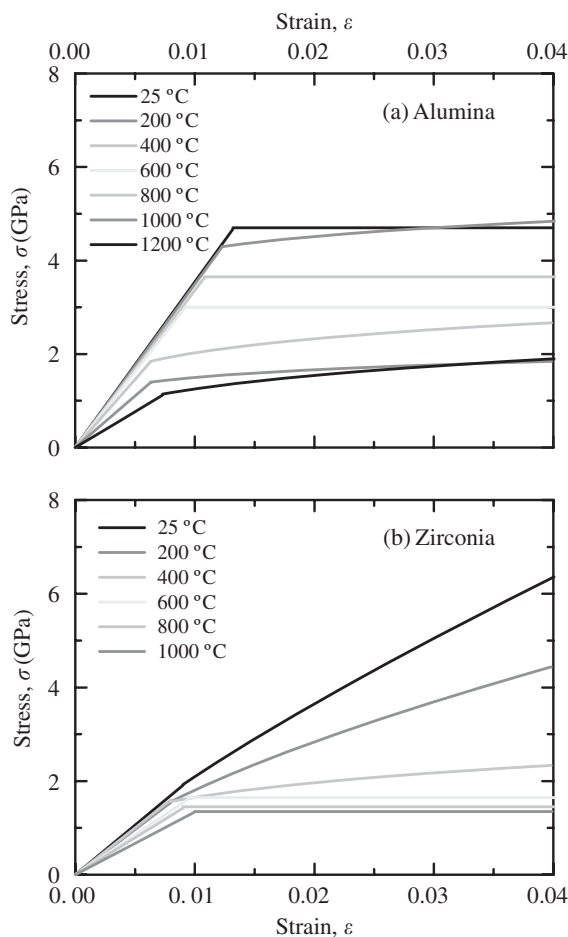


Fig. 6. True stress–strain curves for (a) alumina and (b) zirconia, obtained from data in Figs. 4 and 5 in conjunction with Eq. (2).

tively invariant work-hardening coefficient n in Fig. 5(a). In this case, increasing plasticity is associated with a fast degradation of yield stress. For the zirconia, the curves in the plastic region are much steeper at lower temperatures, leveling out at higher temperatures, reflecting a strongly diminishing n in Fig. 5(b). In this case, the yield stress is more slowly varying. These results suggest basic differences in the underlying plasticity processes in the two materials.

These results raise many interesting issues concerning materials science aspects. However, as already mentioned, the aim of the present paper is to present a methodology to measure mechanical properties at temperatures below the onset of creep. A consideration of underlying material features will be given elsewhere.

Apart from enabling determination of the entire stress–strain curve, the Hertzian methodology is relatively straightforward and economical. Using microscopy to determine contact radii directly in the construction of indentation stress–strain curves (Fig. 3) eliminates errors from thermal or electronic drift that may occur with more instrumented procedures. Measurement errors from thermal contraction of higher temperature indents are small, amounting to less than 1% for materials with expansion coefficients $\approx 10 \times 10^{-6} \text{ K}^{-1}$ and for temperature ranges of $\approx 1000^\circ\text{C}$. It may be argued that the method is cumbersome because it is necessary to perform many individual contacts to produce each full indentation stress–strain curve. However, this can be used to advantage, as it allows one to study the full evolution of contact damage with increasing contact pressure at any given temperature.

Other methods for measuring elastic and plastic properties in ceramics below the creep temperature have been described in the literature. Dynamic testing techniques (e.g., natural resonance

frequency, sound velocity, etc.) are simple, but measure only elastic properties.^{24,25} Uniaxial compression tests are also simple in principle, but are not feasible in most ceramics at lower temperatures because of premature fracture (unless a lateral confinement is imposed).²⁶ Also, uniaxial strain measurements are not easy to make in the elastic region. High-temperature hardness testing machines using Vickers or other sharp indenters are commercially available, enabling routine measurements of hardness H over the same temperature range covered here.^{11–13} However, measurements provide no information on the contribution of elastic modulus E and work-hardening coefficient n to the elastic–plastic response. Instrumented indentation techniques with blunt indenters offer the prospect of determining true stress–strain curves from load–displacement data using a transformation algorithm to compute contact radii,²⁷ but require precision high-temperature displacement measurements, which are subject to thermal and electronic drift.

Apart from its clear application to ceramic materials in general, the indentation methodology technique described here may be extended to more complex high-temperature material systems such as thermal barrier coatings. In such layer systems, it is possible, using FEM, to predict composite responses from stress–strain functions of the individual component materials.²⁸

References

- B. R. Lawn, "Indentation of Ceramics with Spheres: A Century After Hertz," *J. Am. Ceram. Soc.*, **81** [8] 1977–94 (1998).
- A. C. Fischer-Cripps and B. R. Lawn, "Stress Analysis of Contact Deformation in Quasi-Plastic Ceramics," *J. Am. Ceram. Soc.*, **79** [10] 2609–18 (1996).
- F. Guiberteau, N. P. Padture, H. Cai, and B. R. Lawn, "Indentation Fatigue—A Simple Cyclic Hertzian Test for Measuring Damage Accumulation in Polycrystalline Ceramics," *Philos. Mag. A—Phys. Condens. Matter Struct. Defect Mech. Prop.*, **68** [5] 1003–16 (1993).
- A. Pajares, F. Guiberteau, and B. R. Lawn, "Hertzian Contact Damage in Magnesia-Partially-Stabilized Zirconia," *J. Am. Ceram. Soc.*, **78** [4] 1083–6 (1995).
- S. K. Lee, S. Wuttiphon, and B. R. Lawn, "Role of Microstructure in Hertzian Contact Damage in Silicon Nitride. 1. Mechanical Characterization," *J. Am. Ceram. Soc.*, **80** [9] 2367–81 (1997).
- B. R. Lawn, N. P. Padture, H. D. Cai, and F. Guiberteau, "Making Ceramics Ductile," *Science*, **263** [5150] 1114–6 (1994).
- I. M. Peterson, A. Pajares, B. R. Lawn, V. P. Thompson, and E. D. Rekow, "Mechanical Characterization of Dental Ceramics by Hertzian Contacts," *J. Dent. Res.*, **77** [4] 589–602 (1998).
- A. Pajares, L. H. Wei, B. R. Lawn, N. P. Padture, and C. C. Berndt, "Mechanical Characterization of Plasma Sprayed Ceramic Coatings on Metal Substrates by Contact Testing," *Mater. Sci. Eng. A—Struct. Mater. Prop. Microstruct. Process.*, **208** [2] 158–65 (1996).
- H. Y. Liu, B. R. Lawn, and S. M. Hsu, "Hertzian Contact Response of Tailored Silicon Nitride Multilayers," *J. Am. Ceram. Soc.*, **79** [4] 1009–14 (1996).
- M. V. Swain, J. S. Williams, B. R. Lawn, and J. J. H. Beek, "Comparative Study of Fracture of Various Silica Modifications Using Hertzian Test," *J. Mater. Sci.*, **8** [8] 1153–64 (1973).
- C. P. Alpert, H. M. Chan, S. J. Bennison, and B. R. Lawn, "Temperature-Dependence of Hardness of Alumina-Based Ceramics," *J. Am. Ceram. Soc.*, **71** [8] C371–3 (1988).
- V. Tikare and A. H. Heuer, "Temperature-Dependent Indentation Behavior of Transformation-Toughened Zirconia-Based Ceramics," *J. Am. Ceram. Soc.*, **74** [3] 593–7 (1991).
- Y. V. Milman, S. I. Chugunova, I. V. Goncharova, T. Chudoba, W. Lojkowski, and W. Gooch, "Temperature Dependence of Hardness in Silicon-Carbide Ceramics with Different Porosity," *Int. J. Refract. Met. Hard Mat.*, **17** [5] 361–8 (1999).
- S. N. G. Chu and J. C. M. Li, "Impression Creep—New Creep Test," *J. Mater. Sci.*, **12** [11] 2200–8 (1977).
- C. H. Hsueh, P. Miranda, and P. F. Becher, "An Improved Correlation Between Impression and Uniaxial Creep," *J. Appl. Phys.*, **99** [11] (2006).
- J. C. M. Li, "Impression Creep and Other Localized Tests," *Mater. Sci. Eng. A—Struct. Mater. Prop. Microstruct. Process.*, **113513**, **322** [1–2] 23–42 (2002).
- M. V. Swain and B. R. Lawn, "A Study of Dislocation Arrays at Spherical Indentations in Life as a Function of Indentation Stress and Strain," *Physica Status Solidi*, **35** [2] 909–23 (1969).
- K. L. Johnson, *Contact Mechanics*. Cambridge University Press, Cambridge, U.K., 1985.
- P. Miranda, A. Pajares, F. Guiberteau, F. L. Cumbreña, and B. R. Lawn, "Contact Fracture of Brittle Bilayer Coatings on Soft Substrates," *J. Mater. Res.*, **16** [1] 115–26 (2001).
- P. Ludwig, *Element der Technologischen Mechanik*, pp. 32–44. Springer, Berlin, 1909.
- H. Zhao, P. Miranda, B. R. Lawn, and X. Z. Hu, "Cracking in Ceramic/Metal/Polymer Trilayer Systems," *J. Mater. Res.*, **17** [5] 1102–11 (2002).

- ²²P. Miranda, A. Pajares, F. Guiberteau, Y. Deng, and B. R. Lawn, "Designing Damage-Resistant Brittle-Coating Structures: I. Bilayers," *Acta Mater.*, **51** [14] 4347–56 (2003).
- ²³P. Miranda, A. Pajares, F. Guiberteau, Y. Deng, H. Zhao, and B. R. Lawn, "Designing Damage-Resistant Brittle-Coating Structures: II. Trilayers," *Acta Mater.*, **51** [14] 4357–65 (2003).
- ²⁴J. B. Wachtman and D. G. Lam, "Young Modulus of Various Refractory Materials as a Function of Temperature," *J. Am. Ceram. Soc.*, **42** [5] 254–60 (1959).
- ²⁵M. Fukuhara and I. Yamauchi, "Temperature-Dependence of the Elastic-Moduli, Dilational and Shear Internal Frictions and Acoustic-Wave Velocity for

- Alumina, (Y)TZP and Beta'-Sialon Ceramics," *J. Mater. Sci.*, **28** [17] 4681–8 (1993).
- ²⁶W. Chen and G. Ravichandran, "An Experimental Technique for Imposing Dynamic Multiaxial-Compression with Mechanical Confinement," *Exp. Mech.*, **36** [2] 155–8 (1996).
- ²⁷J. S. Field and M. V. Swain, "A Simple Predictive Model for Spherical Indentation," *J. Mater. Res.*, **8** [2] 297–306 (1993).
- ²⁸S. Wuttiphan, A. Pajares, B. R. Lawn, and C. C. Berndt, "Effect of Substrate and Bond Coat on Contact Damage in Zirconia-Based Plasma-Sprayed Coatings," *Thin Solid Films*, **293** [1–2] 251–60 (1997). □